PROCEEDINGS, 41st Workshop on Geothermal Reservoir Engineering
Stanford University, Stanford, California, February 22-24, 2016
SGP-TR-209

Thermal and Geochemical Anomalies in the Eastern Snake River Plain Aquifer: Contributions to a Conceptual Model of the Proposed FORGE Test Site

John A. Welhan

Idaho Geological Survey, Dept. of Geosciences, Idaho State University, Pocatello, Idaho 83209-8072

welhjohn@isu.edu

Keywords: FORGE, ESRP, rhyolite, geochemical tracers, conceptual model

ABSTRACT

Data from the U.S. Geological Survey's National Water Information System (NWIS) database reveal the existence of a number of thermally anomalous areas on the eastern Snake River Plain (ESRP) aquifer, most of them near its margins, and NWIS temperature and chemistry data provided conclusive evidence that thermal waters originating in the hot rhyolitic rocks underlying the ESRP basalts inject heat and solute mass into the overlying ESRP aquifer.

Thermal waters issuing from hot felsic basement rocks in southern Idaho are Na-HCO_3 type due to water-rock reactions at elevated T. They are characteristically depleted in Ca and Mg, typically low in Cl (depending on the source water that reacts with the felsic rock), and high in pH, Na, HCO_3, SiO_2, Li and B (as well as F, if not diluted with high-Ca waters). These diagnostic tracers are seen in thermal waters ($\leq$44 ^{o}C) that issue from shallow wells in late Neogene rhyolites of the Newdale thermal area and thermal waters ($\leq$57 ^{o}C) sampled from INEL-1, a 3.2 km-deep borehole in rhyodacite and welded tuff.

A correlation between SiO_2 and Na/Ca molar ratio appears to be a sensitive indicator of the presence of rhyolite-labeled water, as seen in thermal waters of the Newdale area, the highest-temperature anomaly in ground waters associated with ESRP volcanic rocks, and in dilute mixtures in the ESRP aquifer adjacent to the Newdale area, as well as in warm ground waters of the ESRP aquifer near the INL.

On the INL, contamination from anthropogenic sources and from recharge of both cold tributary surface and ground waters along the aquifer's northern margin renders geochemical tracing of thermal water ineffective in the area of the proposed FORGE test site. The clearest evidence of thermal water entering the aquifer through its base is seen 10-20 km to the southeast where previously identified thermal and geochemical anomalies have been identified, characterized by elevated Na, SiO_2, Li, B and slight enrichments in F, as well as high dissolved He.

An estimate of the advective flux of thermal water in this area was derived via a two-component mixing model. Based on published aquifer flux and porosity information, however, the magnitude of the estimated thermal flux through the base of the aquifer is incompatible with core-scale data on the rhyolite's hydraulic conductivity and vertical gradient observed beneath the INEL-1. This suggests that advective heat transport from the rhyolite is not spatially uniform but focused along localized preferential flow paths within the rhyolite and the mineralized basalts that overlie the rhyolite. This interpretation is consistent with observations of thermal fluid flow in INEL-1's fractured rhyolitic rocks and supports the hypothesis that the rhyolitic basement hosts preferential flow paths.

These findings were incorporated in a geohydrologic conceptual model of the proposed INL FORGE field site.

1. INTRODUCTION

The tremendous geothermal potential of hot rhyolitic rock beneath the eastern Snake River Plain (ESRP) along the track of the Yellowstone hotspot has long been recognized (MIT, 2006), but information necessary for effective exploration and development of this resource, such as its hydraulic characteristics and advective vs. conductive heat transfer mechanisms, has been hard to come by. Except for a very few deep geotechnical and monitoring wells on and near the Idaho National Laboratory (INL) and a few such wells in other locations on the ESRP, too little is known of the rhyolites to effectively constrain its regional thermal structure or our conceptual models of EGS-mineable heat. In the WSRP, for example, a study by Arney et al. (1982) illustrated the relevance of a wide variety of geophysical and geochemical information to assess EGS potential. As part of the Snake River Geothermal Consortium, the Idaho Geological Survey is working on the FORGE initiative to identify an EGS test site on the ESRP. This report the results of an analysis of thermal and geochemical data from the ESRP aquifer that have not previously been evaluated in a geothermal context, in order to refine the geohydrogeologic conceptual model of this thermal resource.

2. GEOHYDROLOGIC BACKGROUND

The ESRP comprises a complex sequence of volcanic materials that record the passage of the Yellowstone hotspot beneath the western North American plate beginning in early to middle Miocene time (Brott et al., 1981). Fractured and highly permeable basalt lava flows of Pliocene and younger age, intercalated with minor amounts of fine to coarse eolian, fluvial and playa sediments, hosts an active, fast-flowing aquifer in the uppermost part of the basalt section (Smith, 2004). Total basalt thickness approaches 2 km in the central portion of the basin, but secondary mineralization has reduced porosity and permeability by orders of magnitude in the deeper basalts (e.g., Morse and McCurry, 2002) and created an effective hydraulic base to the ESRP aquifer. This restricts active ground water flow to the

uppermost ca. 100 to 500 meters of the basalts in the vicinity of the INL (e.g., McLing et al., 2014). Underlying this mineralized aquifer base are more than 3 kilometers of ignimbrite, welded tuff, rhyolitic and granitic basement (hereafter collectively referred to as "rhyolite") that reflect the pervasive silicic volcanism and caldera collapse that occurred in the wake of the hotspot's passage.

Figure 1 depicts some of the many caldera collapse structures that have been postulated to underlie the ESRP basalts (Morgan 1984; Morgan and McIntosh 2005; Drew et al. 2012; Anders et al. 2013). Total volume of erupted felsic material, primarily ignimbrite, has been estimated from 750 km^3 to >1800 km^3 (Morgan and McIntosh, 2005). Although the permeability of these rocks is generally low (e.g., Mann, 1986), intracaldera collapse breccias, ring dikes and fracture zones may be permeable (Branney, 1995; Cole et al., 2005). Deep boreholes that penetrate the rhyolitic rocks beneath the ESRP reveal the existence of open fractures that support active flow zones within otherwise hydraulically "tight" rock (Moos and Barton, 1990; Moody, in press, 2015).

These deep, felsic rocks retain considerable heat, possibly augmented locally by younger heat sources, as expressed in late Quaternary rhyolite domes and crypto-domes of the ESRP. Although the flow of ground water in the basalt aquifer masks high heat flow at depth (e.g., Brott et al., 1981), three quarters of the ESRP's area is thought to exceed 200 ^oC at 4 km depth, making these hot rhyolitic rocks one of the highest-value EGS exploration targets in the U.S. (MIT, 2006; Podgorney et al., 2013; McLing et al., 2014).

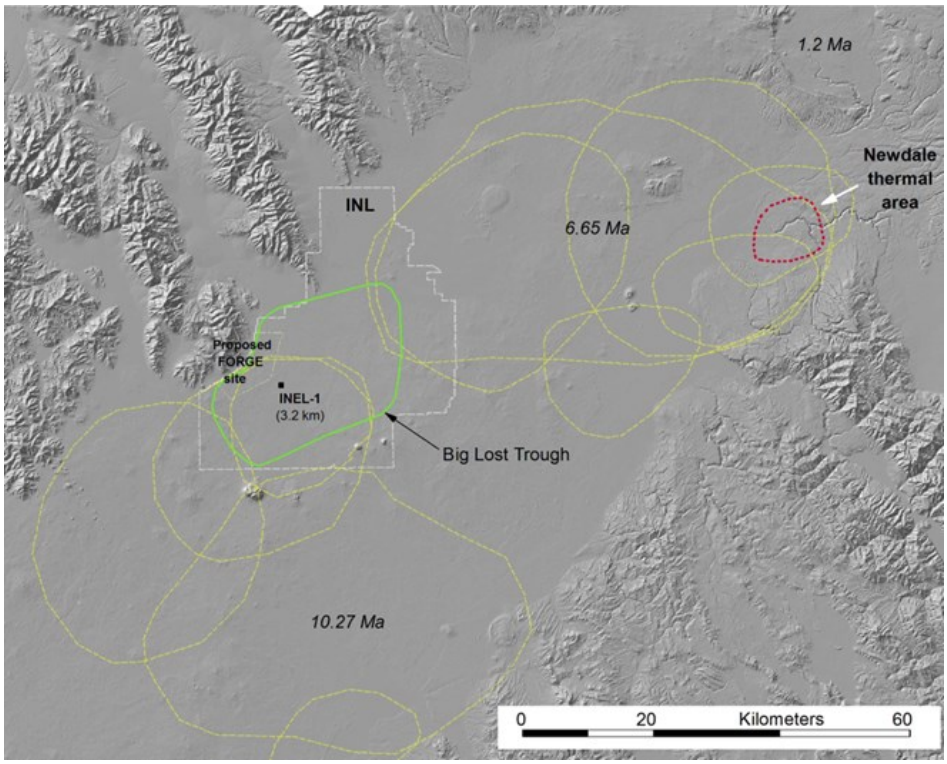

Figure 1: Inferred buried caldera collapse structures beneath ESRP basalts, after M. McCurry (written comm., 2015) based on Morgan (1984); Morgan and McIntosh (2005); Drew et al. (2012); Anders et al. (2013). Area designated as Big Lost Trough represents a long-lived topographic depression that has controlled sedimentation and basalt accumulation for over 0.5 Ma (Bestland et al., 2002), which may be an expression of one or more buried collapse structures in rhyolitic basement rocks.

3. NWIS DATABASE

The USGS's National Water Information System (NWIS) database (http://maps.waterdata.usgs. gov/mapper/index.html) contains a wealth of data on the temperature and chemistry of ground waters in the ESRP aquifer, including trace-element data (**Figure 2**). The data reported on here have not been filtered by well depth, sampling time or aquifer lithology of the producing zone and represent samples collected from individual wells that have been sampled at various times, in some cases spanning a period of decades, by pumping from fixed depths within the aquifer. This report represents a preliminary evaluation of the NWIS data for the purpose of determining whether it sheds useful light on thermal influences in the ESRP aquifer and testable hypotheses with which to constrain geohydrologic conceptual models of the EGS resource beneath the ESRP aquifer.

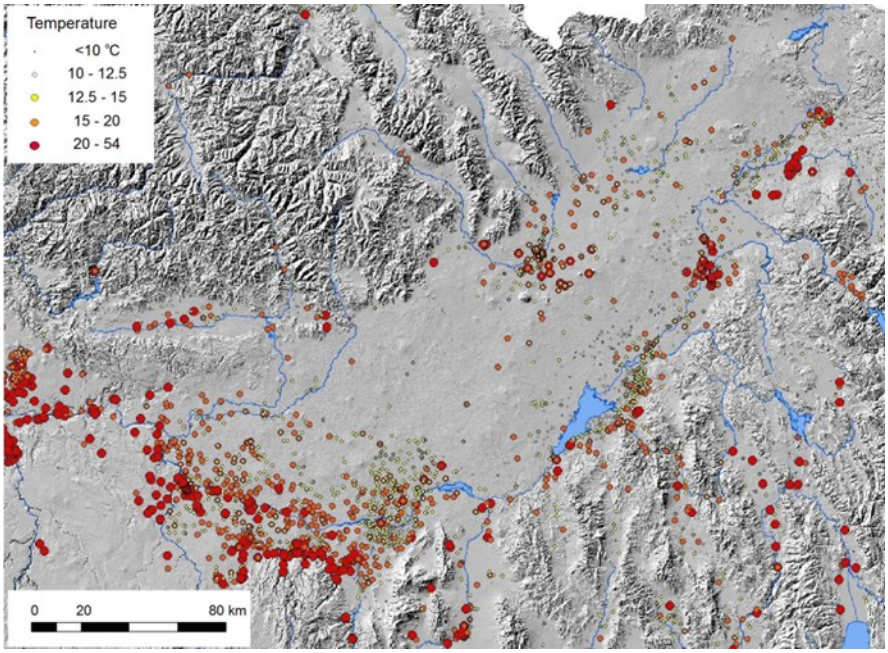

Figure 2: All available temperature data from USGS National Water Information System database for ground waters sampled in southeast Idaho from 1911 to 2015.

3.1. Thermal Data

A number of multi-level sampling systems have been installed on the INL recently, which provide discrete temperature and water quality information from discrete depth intervals within a well (Bartholomay and Twining, 2010). **Figure 3** summarizes all available temperature data from the NWIS data set collected from well Middle 2050A, indicating two important features: (1) pre-2008 data collected by contractors prior to adoption of formal sampling protocols (R. Bartholomay, pers. comm., 2015) shows considerable scatter ($2\sigma \sim 1\ ^{o}C$); and (2) thermal equilibration following drilling, particularly in low-yield and/or infrequently sampled wells could take several years in areas where aquifer permeability or ground water velocities are low. For some wells, therefore, even though measurements were made using standardized protocols, the NWIS temperature data may contain significant uncertainties due to factors such as infrequent or incomplete purging and contributions of water from different depths when sampled under different hydrologic conditions.

The great majority of the ESRP-area wells in the NWIS data set represent ground water from the shallow basalt aquifer; a very small subset of sampled wells represent water issuing from rhyolitic rocks in the Ashton and Newdale areas. As shown in **Figure 4**, the NWIS temperature data define several areas that have ground water temperatures above ambient (defined as ca. 10-12 ^{o}C over most of the ESRP). The tendency of anomalous temperatures to cluster near the margins of the aquifer indicates that the source of this thermal water lies beneath these areas. Whether these thermal manifestations reflect upwelling directly from the underlying hot rhyolitic rocks or whether thermal water rises along structural heterogeneities at the basin margins is not known.

3.2. Regional Geochemical Context

Table 1 summarizes key major and trace-element characteristics of ground water from thermally influenced areas in southern Idaho that reflect the geochemical fingerprint of thermal reaction with felsic rock. Relative to ambient, non-thermal ground water characteristic of the ESRP aquifer, these thermal waters display a striking shift in major-ion composition to Na-HCO_3-type water, with decreased Ca, Mg and increased SiO_2, consistent with thermodynamic predictions of Ramirez-Guzman et al. (2004). They are also greatly enriched in F (indicating they are not influenced by mixing with Ca-rich ground water), as well as Li and B. The fact that thermal waters from the Banbury area are much higher in Cl, while sharing all other characteristics, suggests that the Cl content of the initial reacting water may be a determining factor, as born out by reaction-path modeling (e.g., Ramirez-Guzman, 2004), which shows that the Cl content during reaction with granite remains unchanged.

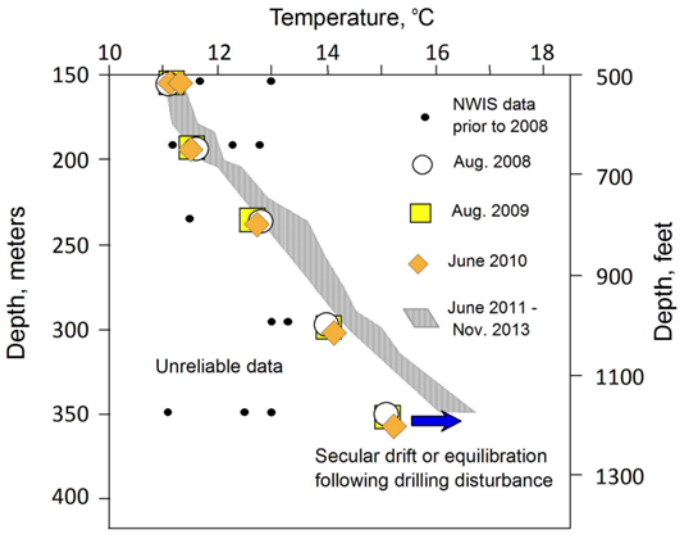

Figure 3: Example of USGS multi-level well temperature data fro well Middle 2050A (drilled 2005), showing poor precision of pre-2008 measurements collected by contractors relative to post-2008 data collected by USGS using consistent sampling protocols. The post-2008 data suggest that thermal equilibration in this well occurred over a time span of at least five years following drilling.

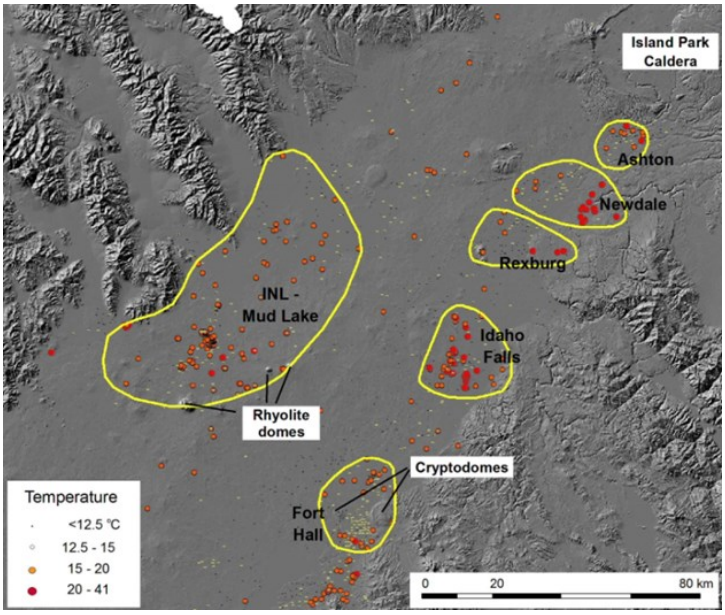

Figure 4: Locations of thermally affected areas in the eastern Snake River Plain aquifer, which may inform on the mechanisms of heat transport from underlying rhyolitic rocks (the EGS resource) into the shallow flow system as well as on the hydraulic characteristics of the resource.

Area			T, °C	pH	Ca	Mg	Na	K	SiO_2	HCO_3	CO_3	SO_4	Cl	F	Li	B	Water Type	Sources
INL rhyodacite (INEL-1 deep borehole)		Mean	48	8.1	8.1	0.9	363	8	85	833		88	14	13	0.29	0.39	$Na\text{-}HCO_3$	Mann, 1986
		2 σ	19	0.4	1.6	1	61	2	30	122		34	5	1	0.01	0.62		
	n = 3	Min	38	7.9	7.3	0.5	330	8	71	780		69	12	12	0.28	0.03		
		Max	57	8.3	8.9	1.1	390	9	101	900		99	17	13	0.29	0.58		
Idaho batholith		Mean	68	9.1	1.8	0.1	82	2	79	54	42	26	9	13	0.08	0.09	$Na\text{-}HCO_3$	Druschel, 1998
		2 σ	32	0.7	2.5	0.1	51	2	37	90	81	23	17	10	0.07	0.11		Krahmer, 1995
	n = 17	Min	42	8.0	0.9	0.0	52	1	46	1	0	10	1	2	0.03	0.02		White, 1967
		Max	88	9.6	6.1	0.2	160	5	105	160	118	45	39	22	0.13	0.20		Young, 1985
																		Youngs, 1981
Boise Front		Mean	76	8.4	1.8	0.1	84	1	58	139		22	7	16	0.04	0.08	$Na\text{-}HCO_3$	Berkeley Group, 1990
		2 σ	14	0.8	1.2	0.1	7	1	26	51		6	6	6	0.02	0.03		Mayo & others 1984
	n = 8	Min	65	7.6	1.3	0.0	79	1	32	110		16	1	12	0.03	0.06		
		Max	88	8.8	3.2	0.1	89	2	78	171		26	11	19	0.05	0.09		
Mountain Home area		Mean	51	9.0	4.5	0.2	85	2	106	128	29	10	8	12	0.01	0.12	$Na\text{-}HCO_3$	Arney et al., 1982
	n = 11	Min	30	7.8	0.9	0.2	52	1	42	50	0	5	2	3	0.00	0.06		
		Max	68	9.6	16.0	0.0	160	5	145	447	49	17	16	20	0.03	0.23		
		2 s	29	1.2	8.3	0.3	57	3	71	236	35	7	8	13	0.02	0.13		
Banbury Hot Springs		Mean	64	9.3	1.1	0.1	130	1	88	67	49	32	40	21	0.05	0.39	$Na\text{-}HCO_3\text{-}Cl$	Lewis and Young, 1982
		2 σ	13	0.4	0.5	0.0	37	0	12	26	16	7	25	12	0.02	0.23		
	n = 7	Min	57	9.0	0.7	0.1	100	1	82	56	35	27	23	14	0.04	0.23		
		Max	72	9.5	1.5	0.1	150	2	100	90	58	35	51	27	0.06	0.51		

Table 2: Summary of major ion and F, Li and B cconcentration (all as mg/l) characteristic of thermal waters in felsic rock environments of the Snake River Plain and Idaho batholith.

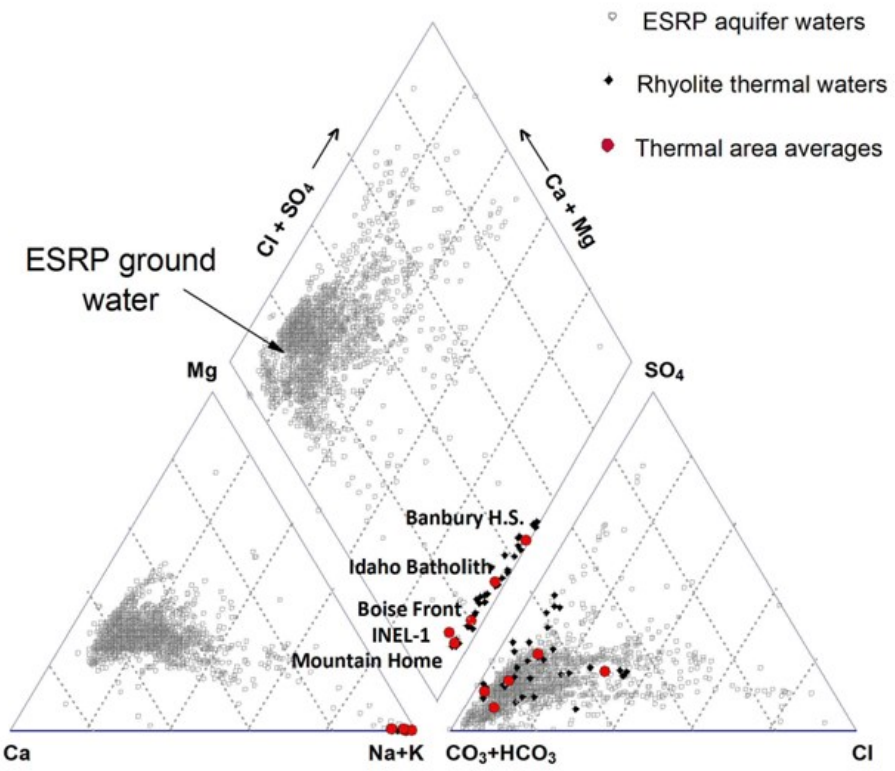

Figure 5: Piper plot summarizing major-ion compositions of ESRP ground water relative to thermal waters that issue from rhyolitic and granitic rocks of southern and central Idaho, which are characteristically depleted in Ca, Mg and enriched in Na, HCO_3, SiO_2 and occasionally Cl, where Cl-rich sedimentary waters have reacted with the hot rock.

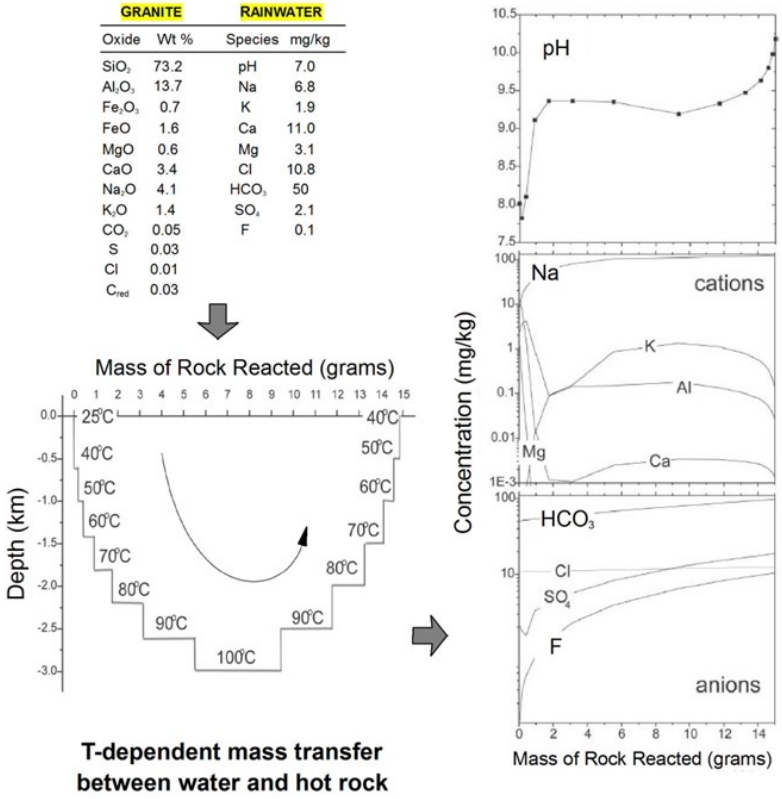

Figure 6: Origin of high-pH, Na-HCO_3-type water as a consequence of a multi-stage reaction path for meteoric water in contact with a granite at elevated temperatures. From Ramirez-Guzman et al. (2004), based on simulations using the CHILLER reaction-path code of Reed and Spycher (1984).

Figure 5 shows general compositional variations in NWIS major-ion data for ground waters of the ESRP aquifer and emphasizes the extreme difference in major-ion composition of thermal waters issuing from hot rhyolitic and granitic rocks of southern and central Idaho, including those adjacent to and that underlie the ESRP aquifer. In general, thermal water-rock reactions between ground waters and these rocks shift the major ion composition away from a Ca-Mg-HCO_3 type that characterizes ESRP ground water toward a strongly Na-HCO_3 composition. As predicted thermodynamically on the basis of reaction-path modeling (e.g., Ramirez-Guzman et al., 2004; **Figure 6**), depletion of Ca^{+2} and Mg^{+2} and enrichment of Na^{+}, HCO_3^{-}, SiO_2, pH and F^{-} are diagnostic of thermal waters that react with granitic rocks. A similar pattern of tracer behavior in thermally affected ground waters of the ESRP would suggest that such waters have interacted with felsic rocks at elevated temperatures and are geochemically so labeled.

3.3. Trace-element Abundances

Thermally anomalous ground waters of the ESRP aquifer (Figures 2 and 4) display certain trace-element enrichments that are diagnostic of thermal waters in contact with felsic volcanic rocks. Enrichments of F, Li and B have been reported in thermal waters of the Idaho batholith as well as in ground waters along the margins of the western SRP (Waag and Wood, 1987; Krahmer, 1995; Druschel, 1998) and have been sampled within the deep borehole, INEL-1, that was drilled into hot rhyolitic rocks beneath the ESRP aquifer (Mann, 1986). Work by Fisher et al. (2012) presented the latest assessment of some of these data in the immediate vicinity of the INL, demonstrating that shallow tributary recharge from the highlands in the vicinity of the aquifer's margins encroaches on and dilutes diagnostic tracers like Li and B in a systematic fashion.

3.4. The Newdale Thermal Area

Figure 7 shows the Newdale thermal area noted in Figure 4, located on the northeastern flank of the ESRP aquifer. In this area, waters up to 44 ^{o}C issue from shallow wells ($\leq$ 300 m) completed in late-Neogene rhyolitic rocks. Ground water in this thermal area serves as a useful end member for evaluating geochemical patterns that arise from high-temperature water-rock reactions with rhyolitic rocks of the ESRP. It also provides a convenient site for examining the low-T waters of the nearby ESRP aquifer for evidence of tracers that could be used to identify thermal water inputs to the aquifer from the adjacent thermal area.

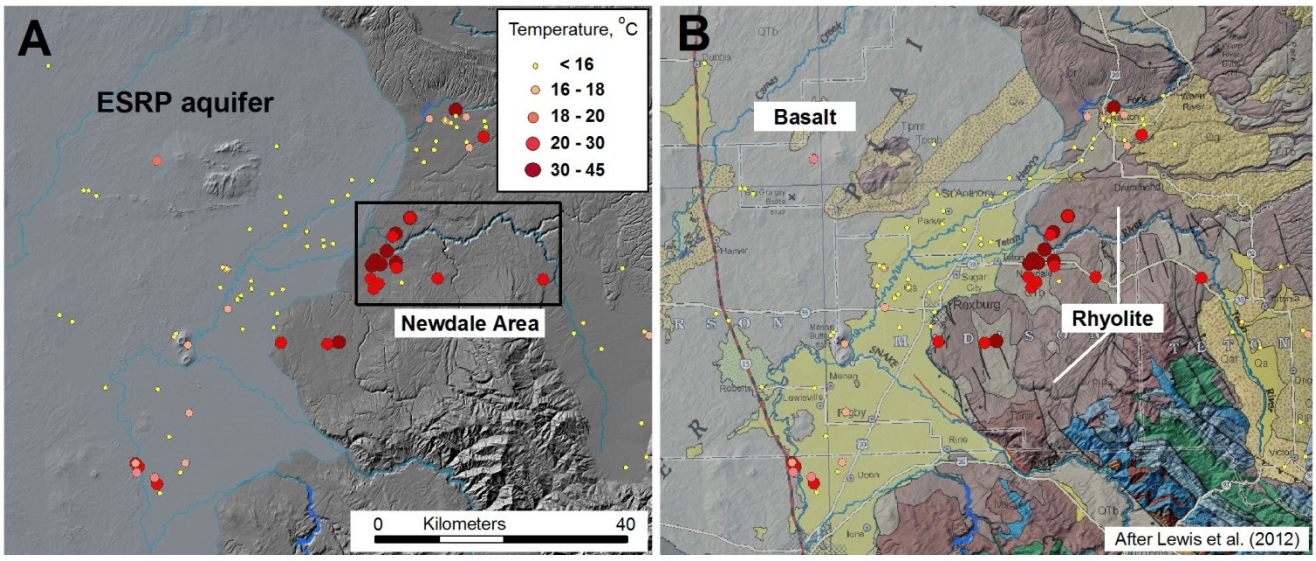

Figure 7: (A) Location of the Newdale thermal area on the northeastern flank of the ESRP aquifer, showing locations of thermal wells completed in late-Neogene rhyolitic rocks of the Heise Group (B). Also shown are locations of low-temperature wells in the ESRP aquifer (A) adjacent to the Newdale area that were evaluated for their tracer patterns and behavior, which might indicate a thermal contribution to ground waters in this part of the ESRP aquifer.

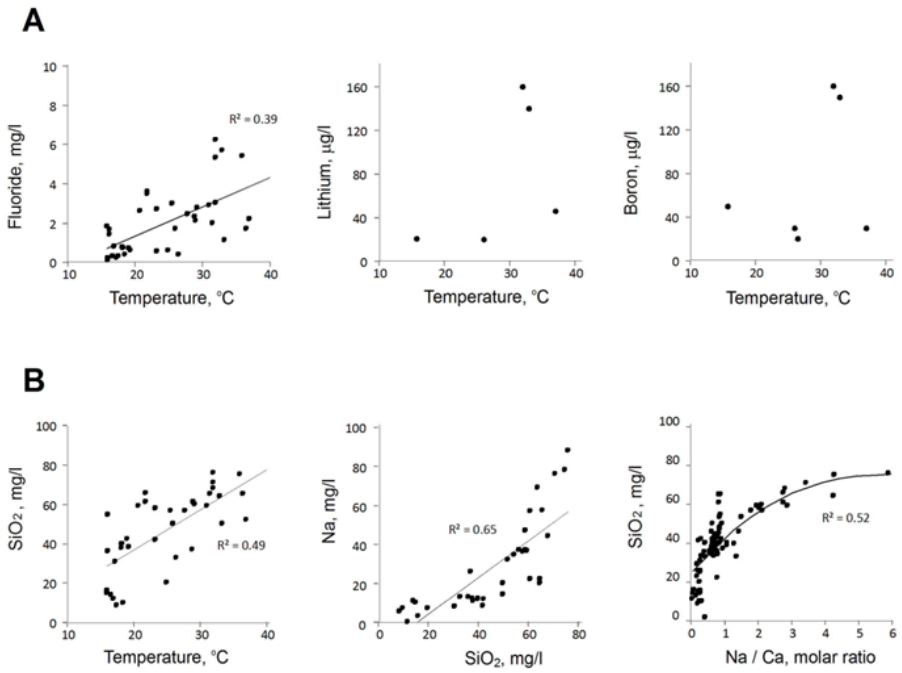

Figure 8: Tracer behavior in thermal well waters of the Newdale thermal area (> 16 ^{o}C), showing key relationships in (A) minor and trace elements and (B) correlations among major elements.

Figure 8 summarizes concentrations of major and minor solutes as reported in the NWIS database for Newdale thermal waters (≥ 16 ^{o}C) that issue from rhyolitic rocks outside the ESRP aquifer. Evidence for rhyolite water-rock labeling is seen in elevated F, Li and B concentrations (Figure 8A), although the data are insufficient to discern any meaningful patterns in Li and B, as well as Na, SiO_2 and Na/Ca ratio. Fluoride concentrations are characteristically limited by fluorite (CaF_2) solubility when Ca^{+2} concentrations exceed 20-30 mg/l in mixtures of Ca-rich ground water.

Figure 9 shows solute tracer behavior in low-temperature (< 16 ^{o}C) ground waters of the ESRP aquifer adjacent to the Newdale thermal are (Figure 7). Note that the correlation of SiO_2 vs. Na/Ca ratios is almost identical to that seen in Newdale's thermal waters (Figure 8) for Na/Ca ratios < 2, suggesting that this correlation may be a sensitive indicator of rhyolite-labeled thermal water where it enters the ESRP aquifer.

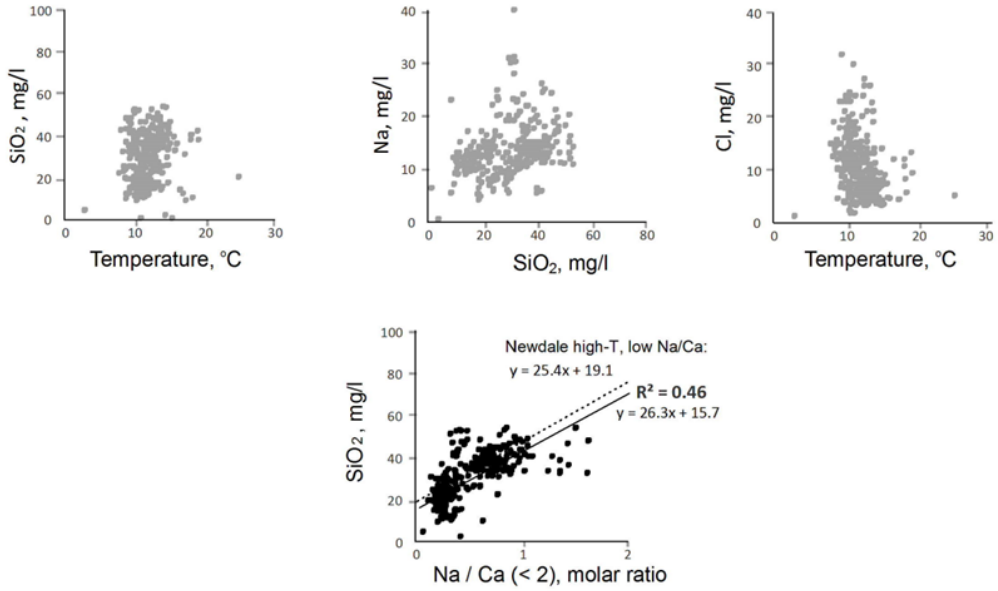

Figure 9: Tracer behavior in low-temperature (< 16 ^{o}C) ground waters of the ESRP aquifer adjacent to the Newdale thermal area. Unlike other solute tracers of rhyolite-labeled thermal waters, which display no useful information (grayed symbol plots), the SiO_2 vs. Na/Ca correlation is almost identical to that observed in Newdale thermal waters in which Na/Ca < 2.

3.5. The Idaho National Laboratory Area

The geochemical patterns observed in the Newdale area are clearly consistent with dilution of rhyolite-labeled thermal water with local Ca-Mg-HCO_3 ground water. In other thermal areas, such as the Rexburg and Ashton areas (Figure 4), high Cl- concentrations observed in the thermal end-member suggest that Cl-rich sedimentary fluids reacted with rhyolitic rock, similar to the Cl-enriched thermal waters of Banbury Hot Springs (Table 1). Even more complex behavior is seen in the Idaho Falls thermal area, with evidence of rhyolite-labeled thermal waters, Cl-enriched thermal waters, and possible anthropogenic water sources (e.g., infiltration from drain wells and canals; Welhan, 2015).

The most complex tracer relationships are observed in wells of the INL thermal area, reflecting local anthropogenic contamination but also mixing processes within boreholes open over a wide depth interval and those that are sampled at multiple depths. **Figure 10**A shows a sitewide plot of 67 samples in which Li correlates with B, and Li correlates with temperature in all but a small subset of samples (Figure 10B); this subset is not site specific and is geographically scattered. Far fewer boron data are available sitewide (not shown), and do not show a correlation with temperature.

Figure 11 summarizes the principal types of Cl vs. T behavior observed in individual INL wells. The majority display essentially isothermal behavior but with large Cl variations (Figure 10B, C). Possible reasons are that Cl is locally introduced from anthropogenic sources (storage ponds, disposal wells, storm water retention basins), and intra-borehole flow in wells open over large intervals may promote mixing of hydrostratigraphic units of different water types (e.g., Bartholomay and Twining, 2010).

4. DISCUSSION

The NWIS data for the Rexburg, Idaho Falls and INL thermal areas indicate that anthropogenic influences as well as water-rock reactions other than with felsic volcanics (e.g., sedimentary rocks) can limit the utility of geochemical tracing. However, where such influences can be ruled out, trace element and temperature information appear to be diagnostic indicators of thermal waters that have originated within the hot rhyolitic rocks of the ESRP.

Table 2 summarizes data on basaltic and felsic rocks from southern Idaho, showing that rhyolitic rocks of the Snake River Plain / Yellowstone volcanic province have much higher Cl and F, elevated Li and slightly higher B compared to SRP basalts, with Cl and F contents in the same range as the granitic rock composition used by Ramirez-Guzman et al. (2004) in their modeling of water-rock interaction (Figure 6). Available B analyses of SRP basalt are very similar to mid-ocean ridge basalt (MORB), whereas the available analyses of evolved basalts at Craters of the Moon show higher B levels, consistent with these rocks' evolved nature.

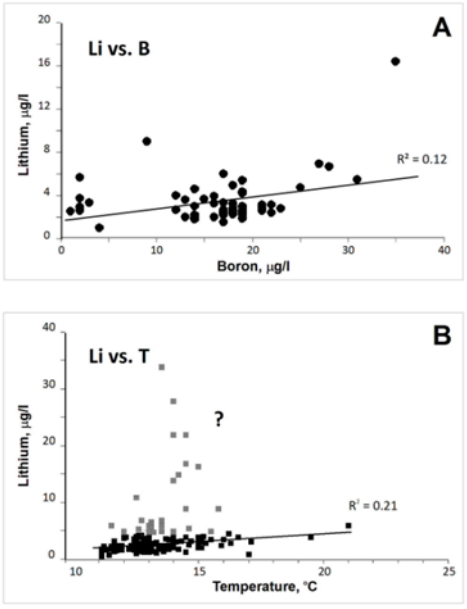

Figure 30: (A) All available NWIS data on Li and B in INL ground waters; far fewer B data (not shown) are available and do not correlate with temperature. (B) Aside from those high Li values shown in grey symbols (possibly reflecting anthropogenic contamination), which exceed the mean of Li values plotted in (A), the great majority of Li concentrations sitewide correlate with temperature at > 99.5% confidence.

Figure 12 depicts the shift in major-ion and trace-element chemistry that occurs in deep borehole INEL-1, a well that was drilled to a depth of 3160 m near the margin of the ESRP, in which rhyodacite and welded tuff comprise the section between 750 m depth and TD (Mann, 1986). These thermal waters also display characteristic major and minor element relationships that reflect thermal reactions with felsic rock, and highlight the striking contrast between these waters and the shallow basalt aquifer (Ca-HCO_3-type above ca. 750 m depth), with very low F, Li. The underlying welded tuff and rhyodacite, in contrast, host a Na-HCO_3-type thermal water considerably enriched in F, Li and B. The step-like change in composition reflects the shift from low-temperature water-rock reactions characteristic of the ESRP aquifer (e.g., Wood and Low, 1988) to reactions with felsic rocks at elevated temperature.

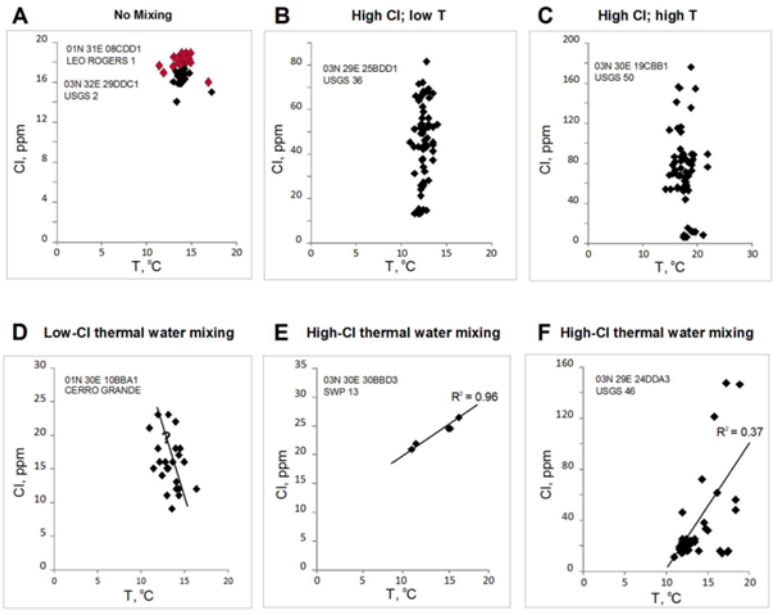

Figure 41: Examples of the most common types of Cl and temperature variability seen in INL-area wells. A minority of wells display no evidence of a mixing relationship (A), whereas the overwhelming majority is characterized by isothermal behavior with large variations in Cl (B, C). Relatively few wells display clear evidence of two-component mixing, such as between ambient ground water with a thermal water having low Cl (D) or elevated Cl (E, F).

			wt. %			ppm				
Rock type	**Sample provenance**		**SiO_2**	**CaO**	**Na_2O**	**Cl**	**F**	**Li**	**B**	**Source**
Basalt, MORB	Famous area, MAR; Tamayo FZ; Juan de Fuca Ridge; EPR; 48 analyses		47.0 - 51.5					5.6 (3 -17)	1.8 (.3-11)	1
Basalt, SRP	Gerritt basalt, Mesa Falls (~ 0.2 Ma)		47.8	11.47	2.35			4.2	1.1	2
" "	Fissure basalt, Spencer Kilgore (~ 0.5 Ma)		44.2	11	2.15			10.2	1.5	2
" "	Kimama flow (15 ka)		45.2	7.5	3.5			21		3
" "	Lava Creek flow, Craters of the Moon (13 ka)		43.5	8.13	3.47			19		3
		Average SRP Basalt	45.2	9.5	2.9	<< 20 *	<< 100 *	13.6	1.3	
Basalt, evolved	Devils Orchard flow, Craters of the Moon (~ 5 ka)		62.1	3.2	4.55			34.4	11.1	2
" "	Highway flow, Craters of the Moon (2.4 ka)		62.9	2.94	4.2			30		3
" "	Serrate flow, Craters of the Moon (2.4 ka)		59.9	3.55	4			30		3
		Average COM Basalt	61.6	3.2	4.3			31.5	11.1	
Rhyolite	Cougar Point tuff, Bruneau-Jarbridge eruptive center (11.5 Ma), three analyse:		74.3	1.1	2.63			29.6	11.2	2
"	Lava Creek Tuff Member B, east of Magic Reservoir (0.64 Ma)		76.9	0.53	3.78			49.6	11	2
"	Big Southern Butte, obsidian (0.3 Ma)		75.9	0.48	4.4			116.7	22.4	2
"	Big Southern Butte, obsidian (0.3 Ma)		74.8	0.47	4.33	2000	2900			4
"	Moonstone Mountain, NW of Magic Reservoir		74.3	0.83	3.43	< 500	2100			4
"	Wedge Butte flow, SE of Magic Reservoir (3.0 Ma)		74.7	0.7	3.94	< 500	4200			4
"	Ammon quarry, ash-flow tuff (4.1 Ma)		71.3	0.99	3.16	< 500	400			4
"	Lost River Range near Howe, vitrophyre		76.5	0.53	3.37		1200			4
"	Nez Perce flow, Yellowstone plateau (0.15 Ma)		76.9	0.49	3.58			41.2	12.5	2
"	Canyon flow, Yellowstone plateau (0.48 Ma)		75.5	0.89	2.7				12.8	2
"	Crystal Springs flow, Yellowstone plateau (70 ka)		76.9	0.49	3.99			74.6	12.5	2
"	Obsidian Cliffs flow, Yellowstone plateau (0.17 Ma)		77.1	0.45	3.93			71.3	12.8	2
		Average SRP Rhyolite	75.4	0.7	3.6	<500	2160	63.8	13.6	
Topaz rhyolite	China Hat flow (57 ka), seven analyses	Topaz Rhyolite **	73.7 ± 5.6	0.7 ± 0.9	4 ± 0.3	380 ± 247	4322 ± 1386	95 ± 18	15 ± 7	5, 6

* inferred from contents of MORB vesicles (Kagoshima et al., 2012)
** mean and 2σ range

1 - Ryan and Langmuir (1987, 1993)
2 - Savov et al. (2009)
3 - Kuntz et al. (1992)
4 - Leeman (1982)
5 - Lewis and Kauffman (2013)
6 - Ford (2005)

Table 2: Comparative summary of available data on F, Li, and B content of basalts and rhyolites of the SRP and vicinity.

4.1. Implications of a Thermal Advective Input

The data from INEL-1 clearly define the geochemical nature of thermal water that has equilibrated with hot rhyolite in one area of the ESRP. The fact that INEL-1's deep thermal water is > 35k years old (Mann, 1986) is consistent with the hypothesis that its Na-HCO_3 composition reflects prolonged reaction with felsic volcanic rocks. The existence of a substantial upward vertical hydraulic gradient between rhyolite and basalt in the areas of INEL-1 (ca. 0.05 - 0.1; Mann, 1986) implies that the hydraulic conductivity of rhyolite and/or mineralized basalts and sedimentary interbeds at the base of the ESRP aquifer must be quite low in order to explain such long residence times. This conjecture is corroborated by hydraulic conductivity measurements which indicate that K < 0.01 m/day in these rocks (Mann, 1986). Even so, Mann (1986) estimated that the flux of these thermal waters into the base of the ESRP aquifer is of the order of 2 x 10^6 m^3/year over the INL's area. If this proves to be typical of other thermally affected areas in the ESRP aquifer, then the magnitude of thermal recharge derived from the rhyolite could comprise a significant fraction of the ESRP aquifer's overall water budget.

4.2. Evidence for Thermal Inputs From Hot Rhyolites

It would be difficult to evaluate such an hypothesis where anthropogenic solutes play a major role, such as on the northwestern half of the INL. Rather, an area of the aquifer that is affected by thermal water inputs but not by anthropogenic disturbances is required. **Figure 13** shows all NWIS wells sampled between 2000 and 2012, together with a kriged interpolation of NWIS temperature data (unfiltered for depth) that are available for the ESRP. The data define a subdued thermal high that extends along the axis of the aquifer southwest of the INL for a distance of more than 80 km. This axial anomaly has persisted in wells sampled post-1995 and therefore is a real feature of the aquifer's thermal structure. Recent heat flow modeling of aquifer temperatures (C. Palmer, unpubl. report, 2015) suggests that this axial thermal feature may be an artifact of low ground water velocities in this area of the aquifer in response to an otherwise geographically uniform basal conductive heat flux.

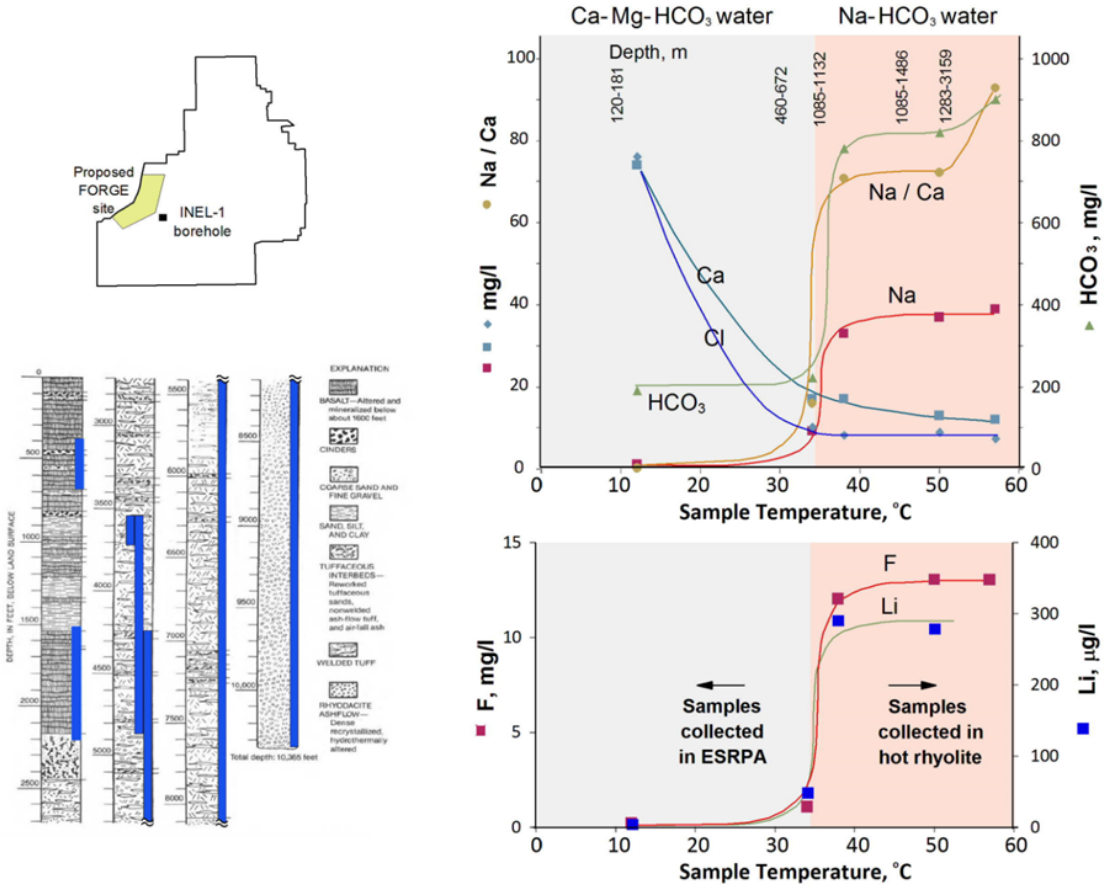

Figure 52: Comparison of thermal waters sampled in deep borehole INEL-1 drilled to 3.2 km in ESRP rhyodacite and welded tuff (Mann, 1986). Major-cation compositional shifts between the ESRP basalt aquifer (Ca-Mg-HCO_3 water type; T ~ 12 °C) and thermal waters in the rhyolitic rocks (Na-HCO_3 water type; T > 30 °C) are accompanied by a 300-fold increase in Na/Ca, a two-fold enrichment in dissolved silica and boron (not shown), and 60-fold enrichments in fluorine and lithium.

As shown in **Figure14**, however, there are areas where ground water temperatures in excess of 14 ^{o}C reflect the input of heat and solute tracers that are characteristic of rhyolite-labeled thermal waters (after Olmsted, 1962; Busenberg et al., 2000, 2001; Fisher et al., 2012). Figure14 summarizes previous work in this regard, showing locations of thermally affected waters beneath the INL as well as areas of anomalous trace solute concentrations that are indicative of rhyolite-labeled thermal waters. These patterns indicate that advective inputs of heat and solute occur in discrete areas of the ESRP where thermal waters enter through the aquifer's base and along its northern margin.

The zone of elevated temperatures along the aquifer's northern margin is heavily influenced by historic waste reprocessing and disposal activities, by dilution with tributary recharge from the highlands outside the aquifer (Olmsted, 1962; Fisher et al., 2012), and by thermal fluid inputs from the northern margin of the aquifer. In contrast, ground waters east of this zone are less diluted by tributary sources and have consistently higher Li , B, F, Na and SiO_2 concentrations. Two areas mapped by Busenberg et al. (2000; 2001) have dissolved He concentrations above air-saturation, which is further evidence for a rhyolitic basement source. The inference is that thermal waters such as those sampled by deep borehole INEL-1 (Figure 12) are injected through the ESRP aquifer's base in these areas.

In Figure 14, a local thermal anomaly identified by Busenberg et al. (2000; 2001) in the southeast corner of the INL has been extended on the basis of NWIS temperature data from additional wells to the southwest, suggesting that Busenberg's thermal anomaly may be part of a much larger axial thermal zone (Figure 13).

Figure 15 summarizes temperature and solute tracer behavior for wells within the axial thermal zone as well as upgradient of it, particularly in the area having enhanced levels of Li, B, F, Na and SiO_2 identified by Busenberg et al. (2000, 2001). As shown in the inset, the low signal/noise contrast in these waters precludes any identification of mixing behavior based on major-ion solutes such as Na and SiO_2. However, the axial thermal zone, as well as ground waters in Busenberg's anomaly (whose dissolved He concentrations are >3 times air-saturation), are characterized by elevated levels of Li and B, with a SiO_2 vs. Na/Ca correlation that is very similar to that observed in the ESRP aquifer adjacent to the Newdale thermal area (Figure 9) and which characterizes Newdale's high-temperature waters (Welhan, 2015).

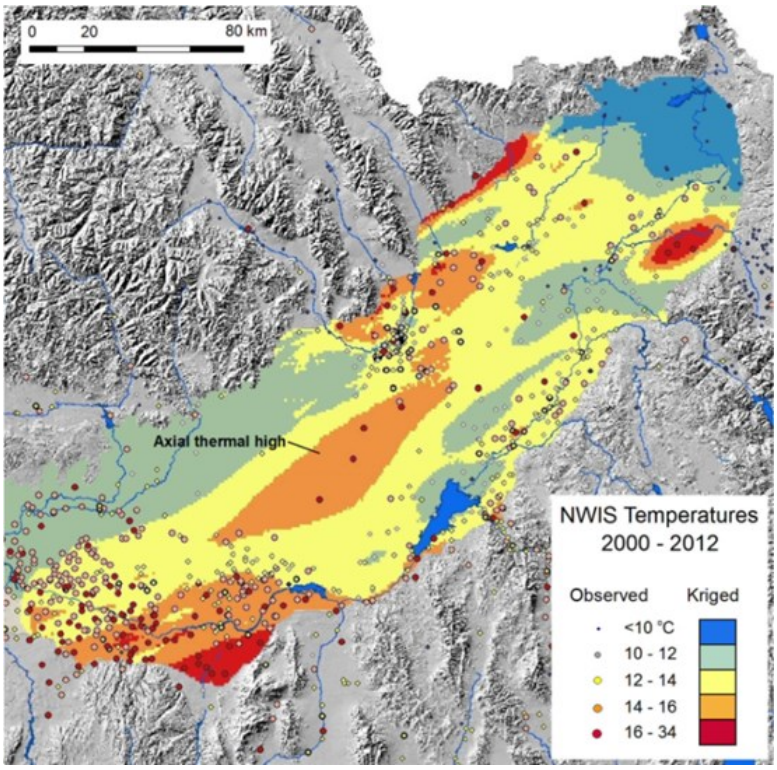

Figure 63: All NWIS temperature data from the period 2000 to 2012 overlain on regional temperature trends as interpolated by ordinary kriging.

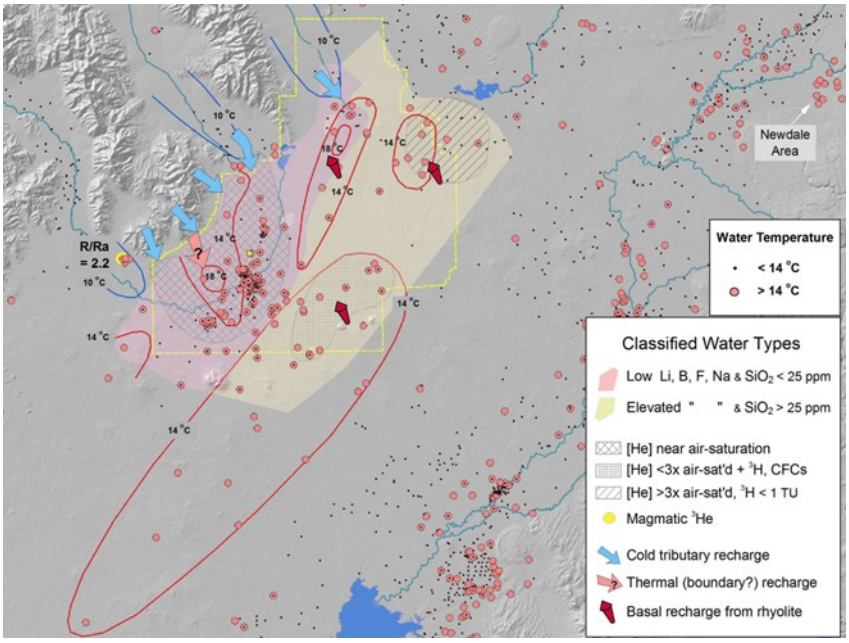

Figure 74: Summary of solute tracer patterns and areas of thermally affected ground waters on the INL, modified after Olmsted (1962), Busenberg et al. (2000; 2001) and Fisher et al. (2012), plotted together with all USGS NWIS data. Helium-isotope (R/Ra) data from Dobson et al. (2015). The area of thermally affected water identified by Busenberg et al. in the INL's southeast corner (stippled) has been extended to include the larger thermal anomaly that extends to the southwest, as indicated in Figure 13.

The pattern of elevated levels of diagnostic tracers in the axial thermal anomaly are summarized in Figure 15: of 24 wells in the axial thermal zone, 17 have T > 14 ^{o}C; 18 have Na above 15 mg/l; 20 have Na/Ca ratios > 0.7; and 11 have Li and B > 10 μg/l and 20 μg/l, respectively. These solute enrichments appear to be confined to the area of this axial thermal anomaly and one identified by Busenberg in the east-central INL area (hatched, in Figure 14). However, well coverage in the intervening area is poor, so it is unclear whether these represent separate thermal anomalies or a larger, contiguous zone of elevated temperatures and tracer concentrations.

Nevertheless, the spatial pattern of solute enrichments that are diagnostic of rhyolite-labeled thermal water indicates that solute mass from the rhyolitic basement is being injected through the base of the aquifer at one or more locations in this area of the ESRP. The spatial distribution of these diagnostic tracers suggest two alternate hypotheses: (1) thermal waters are injected into the ESRP aquifer over a considerable geographic area within and upgradient of the INL; or (2) injection of thermal water and tracer mass is localized where preferential flowpaths exist in the rhyolitic rocks and intervening mineralized basalts that define the base of the ESRP aquifer.

4.3. Advective Heat Transfer

The results of heat transport modeling by Palmer (unpubl. rept., 2015), based on a purely conductive heat-transfer mechanism between the rhyolite and the ERP aquifer, indicate that localized thermal anomalies in the central ESRPA (Figures 13 and 14) are the expression of low-transmissivity zones in the ESRP flow field. That is, aquifer temperatures are higher where ground water flow velocities are low and advective overprinting by shallow ground water flow of basal heat conduction is diminished. However, the model does not consider the implications of advective input of heat, nor can it be used to evaluate whether both conductive and advective heat-transfer processes are operative.

The large vertical hydraulic gradient observed in INEL-1 between the rhyolitic and basaltic flow systems (Mann, 1986) coupled with observations of openly flowing fractures and active thermal water flow in the rhyolite (Moos and Barton, 1990), indicates that a significant advective input of thermal water from the rhyolitic basement is not only possible but needs to be evaluated for a geohydrologic conceptual model.

Corroborating Mann's (1986) hypothesis that a significant advective flux of thermal water through the base of the ESRP aquifer would provide valuable information on the hydraulic connection between the rhyolite and the overlying aquifer as well as the manner in which heat is stored and transported out of the rhyolite. Stated another way, if dilution ratios between ambient ground water and thermal water can be inferred from temperature and/or trace element data, such information would provide an independent estimate of the rhyolite's hydraulic conductivity and the manner in which thermal waters enter the aquifer.

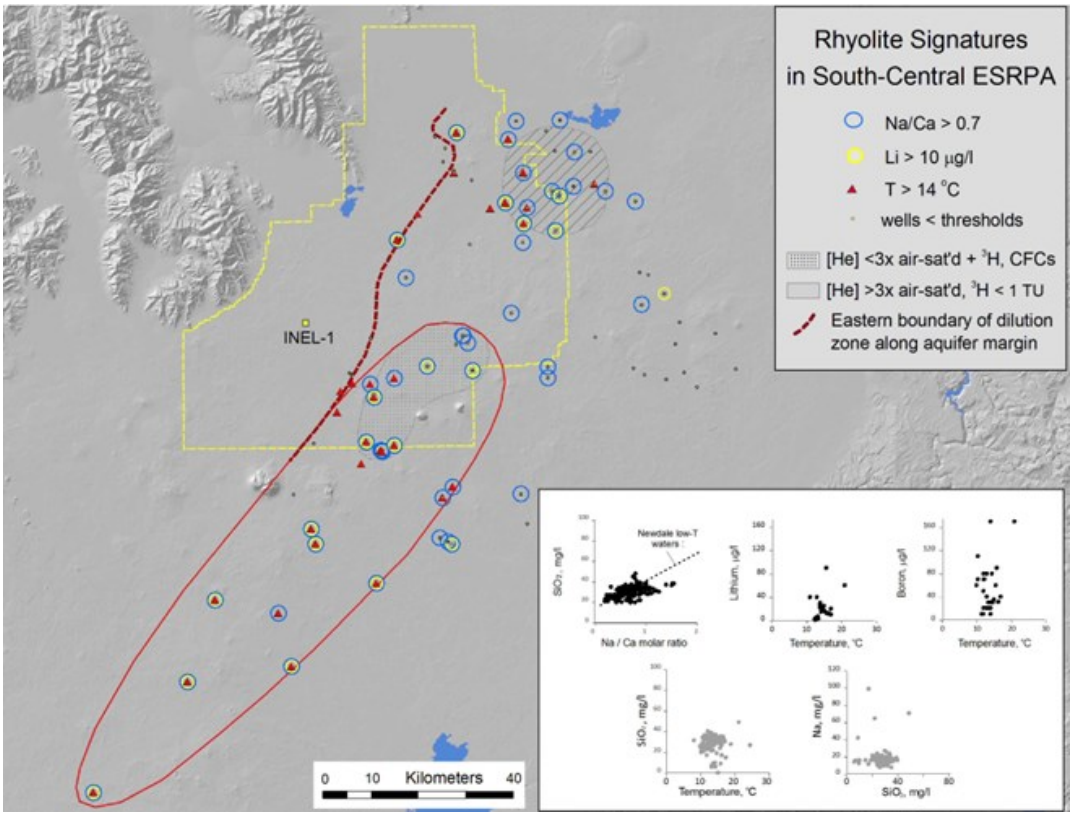

Figure 85: Solute tracer behavior in wells of the axial thermal zone and upgradient wells. The observed SiO_2 vs. Na/Ca correlation is very similar to that seen in the ESRP aquifer adjacent to the Newdale thermal area (Figure 9) and, together with elevated Li and B levels, confirms that rhyolite-labeled thermal water is being advected into the ESRP aquifer in this area.

A two-component mixing model was evaluated in the area of the axial thermal zone (Figure 14), assuming that the chemistry of ground water in the area of the axial thermal high only reflects mixing between regional ESRP ground water and thermal water discharging from the rhyolite.

The average water temperature in wells of the axial thermal zone is 14.9 ^{o}C (2σ = 1.6^{o}; n = 54). **Figure 16** shows all NWIS temperature and Cl data for these wells. In general, the pattern of Cl-temperature variations is reminiscent of that seen in the majority of INL monitoring wells (e.g., Figures 11B, 11C).

The end members in the two-component mixing analysis are: (1) thermal water issuing from the rhyolite beneath the axial thermal zone; (2) local shallow ground water immediately upgradient of the mixing zone; and (3) the composition of the mixture within the mixing zone. To simplify the analysis, mixing between components was assumed to be instantaneous and complete between the base of the aquifer and the sampling depth of each well.

4.3.1 Thermal End Member

Ostensibly, data from INEL-1 would seem to provide a reasonable constraint on the thermal component (Cl = 12 mg/l; Mann, 1986). However, recognizing that its chemical composition and temperatures could be spatially variable, depending on rock type, heat content and water-rock reaction temperature, and the Cl content of ground water that reacts at depth, the best estimate of the maximum Cl composition of thermal water entering the axial thermal zone is assumed to be the minimum Cl concentration shown in Figure 16: ca. 7.5 mg/l. Although lower than INEL-1, it is still well within the range observed in thermal waters that have interacted with felsic rocks in other areas of the SRP (Table 1) and is consistent with INL wells that exhibit mixing behavior with a low-Cl thermal component (e.g., Figure 11D).

The temperature of the thermal end member was defined by the depth to the base of the aquifer where the thermal water enters (ca. 100 m; Podgorney et al., 2013), and INEL-1's thermal gradient (40 ^{o}C/km; Mann, 1986), thereby constraining its temperature at 25 ^{o}C. Information from the nearby Kimama deep borehole (Freeman, 2013) was not considered relevant, because those waters have an unusual Na-Cl composition, and are non-representative of thermal fluids issuing from rhyolite in the INL area.

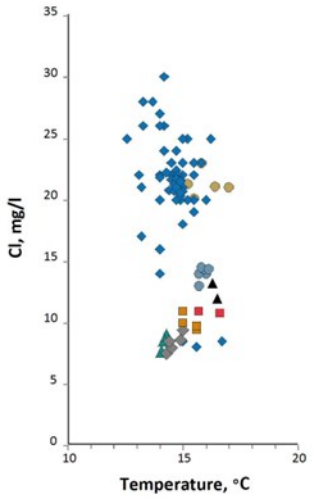

Figure 96: Available Cl-temperature data for wells that define the axial thermal zone south of INL (Figure 14). Data from individual wells are plotted with different symbols.

4.3.2 Non-thermal End Member

The nearest NWIS wells defining upgradient ground water conditions are more than 20 km from the axial thermal zone; more than 70 measurements from such wells within a distance of 60 km have a mean of T = 11.6 ^{o}C (2σ = 3.0) and Cl = 17.6 mg/l (2σ = 30.0). Considering the distances involved and the large relative uncertainties in these averages, however, a better estimate of local ground water flowing through the axial thermal zone was derived from the 119 NWIS analyses of the two highest-Cl wells plotted in Figure 16 with a mean of T = 14.7 ^{o}C (2σ = 1.4) and Cl = 21.2 mg/l (2σ = 8.0). These values are similar to, but somewhat higher than, those defined by the 70 upgradient wells and are considered the best available estimates of the non-thermal end member.

4.3.3 Mixed Water Composition

The thermal water issuing from the base of the aquifer is assumed to mix with ground water moving through the axial thermal zone, a mixture whose composition was estimated from the average of 27 measurements in the lowest-Cl wells shown in Figure 13: T = 15.6 ^{o}C (2σ = 1.5) and Cl = 10.3 mg/l (2σ = 6.0). Note that the 60% relative uncertainty in this Cl estimate renders any mixing calculation highly uncertain.

With the above estimates in hand, the mixing fractions of the thermal and non-thermal end members can be determined using the following relationship (for temperature):

$$T_{mix} = f * T_{thermal} + (1\text{-}f) * T_{non\text{-}thermal}, \quad (1)$$

where T_{mix} = 15.6 ^{o}C, $T_{thermal}$ = 25 ^{o}C, $T_{non\text{-}thermal}$ = 14.7 ^{o}C, and f is the mixing fraction of thermal water flux relative to the diluting flux of ESRP ground water, defined as $Q_{thermal}/(Q_{thermal} + Q_{non\text{-}thermal})$, where $Q_{thermal}$ is the specific vertical Darcy flux (per m^2) defined by the hydraulic conductivity (K) and vertical gradient (I) within the rhyolitic rocks:

$$Q_{thermal} = K_{rhyolite} * I_{rhyolite}. \quad (2)$$

Solving for f in equation (1) yields an estimate of the mixing fraction based on temperature. In this case, f = 0.087; i.e., $Q_{thermal}$ is an order of magnitude smaller than $Q_{non\text{-}thermal}$. In comparison, the flux ratio estimated using Cl data is unreasonably large, being almost an order of magnitude greater (f = 0.82). Given the large relative uncertainties in the estimated T and Cl end member values, such a discrepancy is not unexpected.

4.4. Inferred Hydraulic Conductivity of Rhyolite

Based on linear tracer velocities and porosities (0.05-0.2) for basalts in the vicinity of the axial thermal zone, Ackerman et al. (2006) estimated the specific Darcy flux in the aquifer, $Q_{non\text{-}thermal}$, to be in the range of 1.5 to 13 m/day. Mann (1986) estimated a vertical hydraulic gradient of 0.07 m/m in the upper part of INEL-1. Assuming the vertical gradient beneath the axial thermal zone is in the range of 0.05 to 0.1 m/m, then the flux ratio estimated via f in equation (1) and the specific Darcy flux in the ESRP aquifer allows $K_{rhyolite}$ to be estimated using equation (2). The estimated range of $K_{rhyolite}$ is therefore 1.5 to 25 m/day.

This estimate is orders of magnitude larger than the hydraulic conductivity reported for unfractured rhyolite in borehole INEL-1 (0.0005 to 0.01 m/day; Mann, 1986). The only way to reconcile these disparate results is to conclude that either (i) the flux ratio derived on the basis of temperatures is grossly inaccurate or (ii) the thermal flux into the aquifer is localized and focused along preferential flow paths

having a much higher effective hydraulic conductivity, such as in large fracture zones, zones of collapse breccias associated with buried caldera structures, and/or vertical heterogeneities along the feeder dikes of Big Southern Butte and nearby rhyolite domes.

Possibility (i) cannot be ruled out, because flux ratios < 0.01 apply to scenarios where $T_{thermal} >> 25\ ^{o}C$ and/or $T_{non\text{-}thermal}$ is very close to T_{mix}. Possibility (ii) could apply to either or both the fractured rhyolite and/or mineralized basalt that overlies the rhyolite and defines the base of the ESRP aquifer. The colored underlay in **Figure 17**, taken from Whitehead (1986), represents interpreted basalt thickness based on resistivity data; since basalt outcrops at or near the surface in this part of the ESRP, its thickness can be used as a first-order proxy for depth to rhyolite. Note that the axial thermal high in Figure 17 originates near where rhyolite appears to shallow to within 300-600 m of the surface before deepening rapidly to the northeast, south and southwest. This fact alone could facilitate the transport of thermal water into the shallow aquifer at this location.

The clustered nature of thermal occurrences on the ESRP (Figure 4), therefore, may be a reflection of thermal outflow from rhyolitic basement rocks along preferential flow paths associated with buried caldera collapse structures that are inferred to underlie the ESRP (Figure 1), and is also consistent with the highly fractured nature of rhyolitic rocks beneath the Snake River Plain that have been drilled. For example, Moos and Barton's (1990) analysis of INEL-1's high-resolution televiewer log confirmed that fracture density varies considerably in different depth zones, that large-aperture fractures exist in the rhyolite, and even though most fractures are sealed due to past hydrothermal deposition, open fractures do exist and are associated with elevated temperatures that indicate active flow of thermal water. Together with the inferences made from the mixing calculation, these facts suggest that thermal water, that is actively circulating within the rhyolite, makes its way into the ESRP aquifer only in certain areas, possibly where the rhyolite is shallowest and/or where local preferential flow paths channel thermal water into the shallow aquifer. This may explain the geographically localized nature of thermal ground water occurrences in the ESRP aquifer (Figure 4).

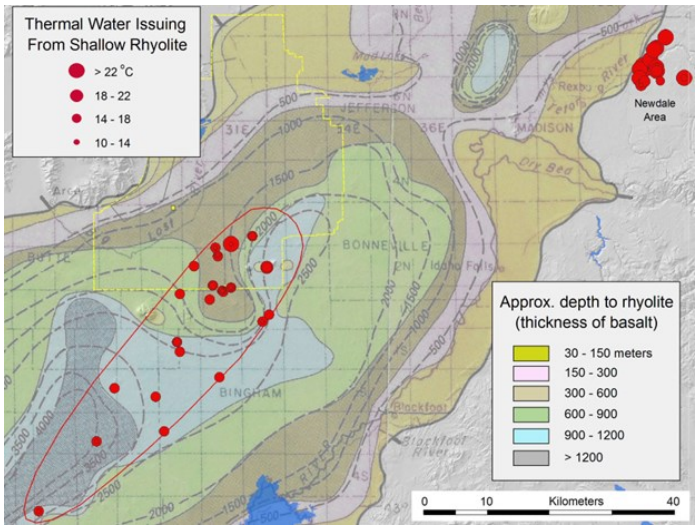

Figure 107: Wells that define the axial thermal zone in the vicinity of the southern INL. The colored underlay, taken from Whitehead (1986), represents interpreted basalt thickness based on resistivity data and deep control wells; it serves as a proxy for depth to rhyolite/mineralized basalt (contours are in feet).

5. GEOHYDROLOGIC CONCEPTUAL MODEL

The NWIS geochemical and temperature data examined in this study lead to some significant inferences and conclusions. **Figure 18**, adapted from Mcling et al. (in press), depicts the current working hypothesis: the head of the axial thermal zone coincides with the area where the conductive gradient in altered basalts and underlying rhyolite shallows considerably, which is consistent with the inference based on Figure 17's basalt thickness / depth to the base of the aquifer. The figure also underscores the complex nature of the aquifer's northern margin where both thermal and non-thermal tributary inputs (including possible fault-controlled upwelling) and their corresponding geochemical signatures can complicate interpretations of mixing.

Figure 19 summarizes essential elements of the geohydrologic conceptual model, which incorporates the geochemical information and constraints identified in this work. The key elements of the model are:

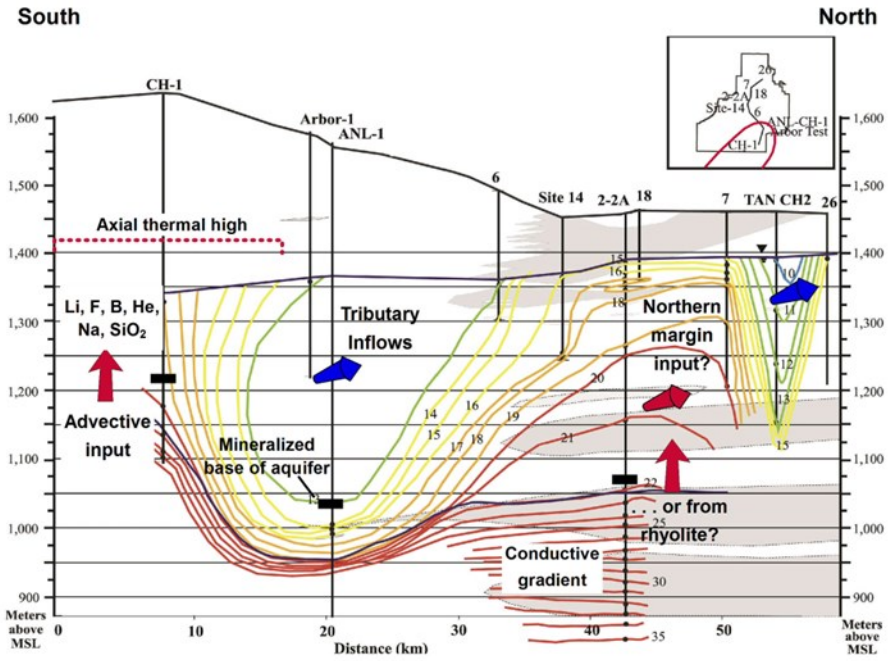

Figure 118: Cross section from north to south showing isotherms (°C) in the ESRP aquifer beneath the INL, the base of the aquifer (mineralized basalt / rhyolite and the depth of conductively dominated heat flow), and inferred fluxes of thermal and non-thermal into the aquifer from its northern margin and from the underlying rhyolite. Red arrows represent, thermal water inputs through the base of the aquifer as well as possible fault-controlled upwelling along the aquifer's margin, and blue arrows represent cold ground water / surface water inflows from the ESRP's bounding highlands and tributary valleys. The position of the axial thermal anomaly of Figure 17 is indicated in the inset.

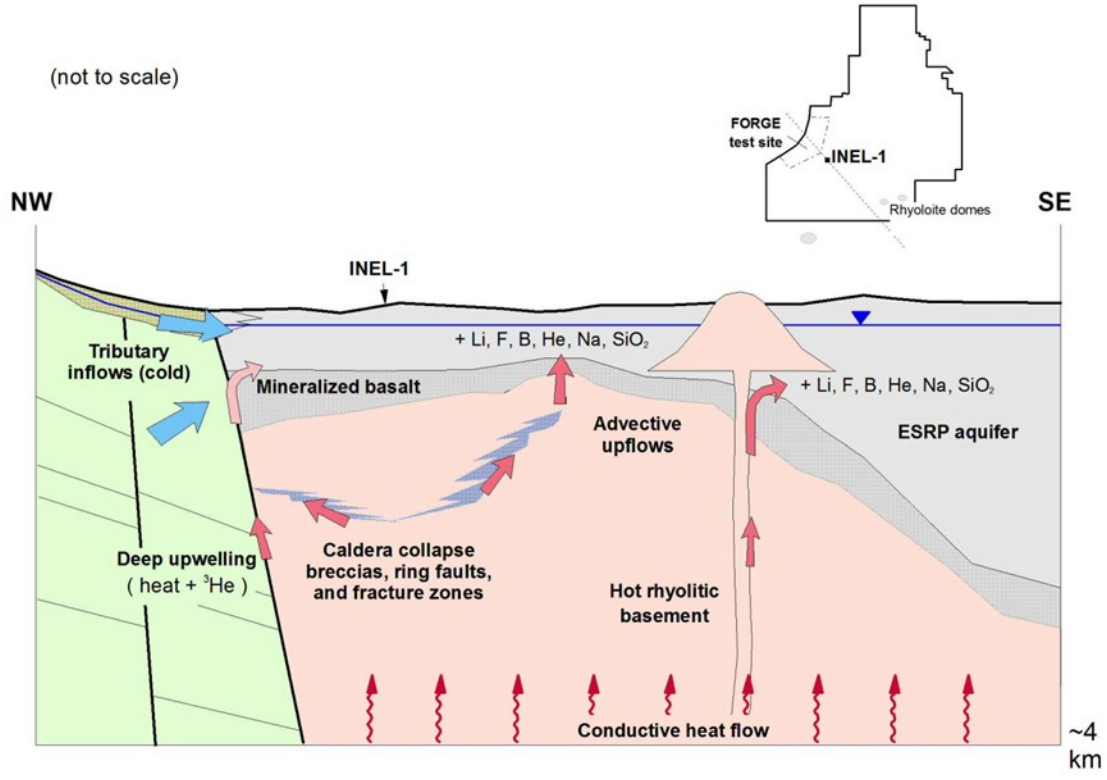

Figure 129: Conceptual model of ESRP geohydrology in the vicinity of the proposed FORGE test site, illustrating key elements controlling advective heat and solute inputs to the ESRP aquifer.

- Conductive heat flow raises aquifer water temperatures in low-velocity zones
- Heat and solute tracers from rhyolitic basement are injected into the aquifer's base
- Thermal and non-thermal advective inputs (heat + tracers) occur at the aquifer margin
- Preferential flow zones in the rhyolitic basement and the mineralized base of the aquifer focus these advective thermal inputs to the aquifer

Steady-state heat transport modeling indicates that ESRP aquifer temperatures are sensitive to the ground water velocity field (C. Palmer, per. comm., 2015). Assuming purely conductive heat transfer at the base of the active flow regime, elevated water temperatures are predicted a considerable distance above the base of the aquifer in areas where local ground water velocities are low. This builds on previous work (e.g., Brott et al., 1981; Blackwell, 1989) and confirms that conductive heat transfer exerts an important first-order control on the thermal state of the ESRP aquifer.

As Welhan (2015) has suggested, and the preceding analysis confirms, the association of elevated temperatures with the presence of certain major and trace elements in thermal ground waters of the ESRP is a characteristic feature of these waters. In particular, enrichments in Na, SiO_2, Li and B appear to be diagnostic of thermal water-rock reactions in the rhyolitic basement rocks and provides conclusive evidence that advective heat transport must be considered in any conceptual model of the deep EGS resource.

Work by Busenberg et al. (2000, 2001) has shown that these same elements, as well as dissolved He, are enriched in areas of the INL where above-ambient ground water temperatures are found, corroborating the hypothesis that rhyolite-labeled thermal waters are injected through the base of the aquifer in the area of the INL. Their work also suggests that thermal waters are injected into the aquifer at the aquifer's northern margin, perhaps along basin-bounding fault structures. Measurements by Dobson et al. (2014) of elevated 3He/4He ratios in a nearby thermal well corroborates the hypothesis that heat and solute mass from depth are injected along the aquifer margin. However, due to extensive dilution by tributary surface and ground waters in this area of the aquifer, it is not known whether these thermal waters also are enriched in rhyolite-derived solutes.

The most speculative element of the conceptual model portrayed in Figure 19 is the mechanism by which thermal water moves within the rhyolitic basement and makes its way to the overlying aquifer. The results of the two-component mixing model suggest that the axial thermal zone is supported by localized preferential flow. To date, the generation of permeable structures created by caldera collapse has focused on structures and lithofacies inferred from theoretical and experimental models (e.g., Branney, 1995; Cole et al., 2005) that have led to new insights into collapse mechanisms and resulting structures. Acocella (2008) proposed a four-stage, subsidence-controlled collapse sequence resulting in a series of nested calderas bounded by normal and reverse ring faults and intra-caldera collapse breccias. Together with permeable fault and fracture zones, these breccia facies may be particularly important in determining the geometry of preferential flow within the rhyolitic basement rocks.

6. IMPLICATIONS FOR EGS DEVELOPMENT

The scale of advective transport within the rhyolite basement is not known, but its existence raises the possibility that the thermal resource in the FORGE target zone may be significantly affected by hydrothermal heat transfer. Also, if preferential flow proves to be an important factor in this area and heterogeneous facies such as collapse breccias play a major role, then issues like rock strength, stress conditions and impacts on drilling and fracture stimulation in a highly fractured rock environment may need to be considered.

Finally, given the sharp contrast in chemical compositions of ESRP ground water and fluids that are expected to be encountered in the EGS target rocks, consideration should be given to the thermodynamic stability of the solute load in shallow ground water if it is used as the heat-transfer fluid. In addition, its potential to cause Ca-scaling problems due to $CaCO_3$ and CaF_2 must be evaluated and chemical necessary stabilization approaches identified.

7. CONCLUSIONS

Certain solutes found in anomalously warm ground waters of the ESRP aquifer are diagnostic of thermal water-rock reactions in rhyolitic / felsic rocks. Enrichments in Na, SiO_2, Li and B, in particular, are diagnostic indicators of the presence of rhyolite-labeled thermal water, as might high dissolved He concentrations (Busenberg, 2001) and diagnostic proportions of SiO_2 vs. Na/Ca, which appears to be a sensitive indicator even in highly dilute mixtures. The association of these tracer solutes with elevated ground water temperatures that occur in spatially discrete clusters throughout the ESRP conclusively demonstrates that heat transfer into the ESRP aquifer occurs not only via conduction but by advection of heat and solutes through its base and at its margins.

The failure of a simple two-component mixing model to independently confirm the magnitude of core-scale rhyolite hydraulic conductivity measurements in INEL-1 may simply reflect the low signal/noise contrast in thermally affected areas of the aquifer and uncertainty in the values of the end-member temperatures used in the mixing calculation. Significant spatial variability in the vertical hydraulic gradient and/or the magnitude of the lateral Darcy flux in the ESRP aquifer could also be responsible. On the other hand, it may indicate that considerable permeability heterogeneity exists and that preferential flow paths dominate advective transport in the rhyolites. This is supported by the observed association of thermal fluid flow in open fractures in INEL-1 (Moos and Barton, 1990), as well as more recent data on fracture geometry in deep boreholes drilled into rhyolite in other parts of the Snake River Plain (Shervais et al., 2013; Moody et al., in prep.), which indicate that open fractures and systematic changes in fracture density with depth will need to be considered in assessments of hydraulic conditions within the EGS resource.

ACKNOWLEDGEMENTS

I thank Rob Podgorney and Tom Wood for arranging INL-LDRD project funding and for their support of this work. Discussions with Mitch Plummer and Carl Palmer on their conductive heat flow modeling results proved very helpful in wrapping up this analysis, and Pat Dobson and Mike McCurry provided very helpful comments on helium and caldera collapse structures, respectively.

REFERENCES

Ackerman, D.J., G.W. Rattray, J.P. Rousseau, L.C. Davis and B.R. Orr, 2006, A conceptual model of ground-water flow in the eastern Snake River Plain aquifer at the Idaho National Laboratory and vicinity with implications for contaminant transport; U.S. Geological Survey, Sci. Investigations Rept. 2006-5122, 62 pp.

Acocella, V., 2008, Structural development of calderas: A synthesis from analogue experiments, Caldera Volcanism: Analysis, Modelling, and Response, p. 285-311.

Arney, B.H., F. Goff and Harding–Lawson Associates, 1982, "Evaluation of the hot dry rock geothermal potential of an area near Mountain Home, Idaho," Los Alamos National Laboratory Report LA-9365-HDR, 65 pp.

Bartholomay, R.C. and B. V. Twining, 2010, Chemical Constituents in Groundwater from Multiple Zones in the Eastern Snake River Plain Aquifer at the Idaho National Laboratory, Idaho, 2005-08; U.S. Geological Survey, Sci. Investigations Rept. 2010-5116, 82 pp.

Berkeley Group, 1990, Boise geothermal aquifer study; Idaho Dept. of Water Resources, Final Report, DOE/ID/12748-3, 119 pp. plus appendices.

Branney, M.J., 1995, Downsag and extension at calderas: new perspectives on collapse geometries from ice-melt, mining, and volcanic subsidence; *Bulletin of Volcanology*, v. 57, p. 303-318.

Brott, A., D.D. Blackwell, and J.P. Ziagos, 1981, Thermal and tectonic Implications of heat flow in the eastern Snake River Plain: *Journal of Geophysical Research*, v. 86, p. 11,709–11,734.

Busenberg, E., L.N. Plummer, M.W. Doughten, P.K. Widman and R.C. Bartholomay, 2000, Chemical and isotopic composition and gas concentrations of ground and surface water from selected sites at and near the Idaho National Engineering and Environmental Laboratory, Idaho, 1994 through 1997: U.S. Geological Survey Open-File Report 00–81 (DOE/ID–22164), 51 p.

Christiansen, E.H., M.F. Sheridan and D.M. Burt, 1986, The Geology and Geochemistry of Cenozoic Topaz Rhyolites from the Western United States: *Geol. Soc. Am. Special Paper* 205, 82 pp.

Cole, J.W., Milner, D.M., and Spinks, K.D., 2005, Calderas and caldera structures: A review; Earth-Science Reviews, vol. 69, p. 1-26. Druschel, G.K., 1998, Geothermal systems in the Idaho batholith: Geology and geochemistry; Washington State University, M.S. thesis, 183 pp.

Dobson, P.F., B.M. Kennedy, M.E. Conrad, T. McLing, E. Mattson, T. Wood, C. Cannon, R. Spackman, M. van Soest and M. Robertson, 2015, *Proceedings*, 40th Workshop on Geothermal Reservoir Engineering, Stanford University, Stanford, California, SGP-TR-204, 7 pp.

Fisher, J.C., J.P. Rousseau, R.C. Bartholomay and G.W. Rattray, 2012, A comparison of U.S. Geological Survey three-dimensional model estimates of groundwater source areas and velocities to independently derived estimates, Idaho National Laboratory and vicinity, Idaho; U.S. Geological Survey, Sci. Investigations Rept. 2012-5152, 130 pp.

Ford M.T., 2005, The petrogenesis of Quaternary rhyolite domes in the bimodal Blackfoot Volcanic Field, southeastern Idaho: M.S. thesis, Idaho State University, 133 pp. plus one plate.

Freeman, T.G., 2013, Evaluation of the geothermal potential of the Snake River Plain, Idaho, based on three exploration holes; Utah State University, M.S. thesis, 90 pp.

Johnson, T. M., R.C. Roback, T.L. McLing, T.D. Bullen, D.J. DePaolo, C. Doughty, R.J. Hunt, R.W. Smith, L.D. Cecil and M.T. Murrell, 2000, Groundwater "fast paths" in the Snake River Plain aquifer: Radiogenic isotope ratios as natural groundwater tracers; *Geology*, v.28, p.871-874.

Kagoshima, T., N. Takahata, J. Jung, H. Amakawa, H. Kumagai and Y. Sano, 2012, Estmation of sulfur, fluorine, chlorine and bromine fluxes at Mid-Ocean Ridges using a new experimental crushing and extraction method; *Geochem. Journal*, v.46, p.21-26.

Krahmer, M.S., 1995, The geology and geochemistry of the geothermal system near Stanley, Idaho; Washington State University, M.S. thesis, 169 pp.

Kuntz, M.A., H.R. Covington and L.J. Schorr, 1992, An overview of basaltic volcanism of the eastern Snake river Plain, Idaho; in P.K. Link, M.A. Kunz, and L.B. Platt (eds.), Regional Geology of Eastern Idaho and Western Wyoming, *Geol. Soc. America, Memoir* 179, p.227-267.

Leeman, W.H., 1982, Rhyolites of the Snake River Plain-Yellowstone Plateau Province, Idaho and Wyoming: A summary of petrogenetic models; in B. Bonnichsen and R. Breckenridge (eds.), Cenozoic Geology of Idaho, p.203-212.

Lewis, R.S., P.K. Link, L.R. Stanford and S.P. Long, 2012, Geologic map of Idaho: Idaho Geol. Survey Geologic Map 9, scale 1:750,000.

Lewis, R.S. and J.D. Kauffman, 2013, Selected radiometric and analytical data for the China Hat Dome area, NURE Project, southeastern Idaho: Idaho Geological Survey Digital Analytical Data Series DAD-9.

Lewis, R.E. and H.W. Young, 1982, Thermal springs in the Payette River basin, west-central Idaho; U.S. Geological Survey, Water Resources Investigations Rept. 80-1020, 23 pp. plus plates.

Mann, L.J., 1986, Hydraulic properties of rock units and chemical quality of water for INEL-1: A 10,365-foot deep test hole at the Idaho National Engineering Laboratory; U.S. Geological Survey, Water Resources Investigations Rept. 86-4020, 23 pp.

Mayo, A.L., A.B. Muller and J.C. Mitchell, 1984, Geochemical and Isotopic Investigations of Thermal Water Occurrences of the Boise Front Area, Ada County, Idaho; Idaho Dept. of Water Resources, *Water Information Bull.* No. 30, Part 14, Geothermal Investigations in Idaho, 55 pp.

McLing, T., McCurry, M., Cannon, C., Neupane, G., Wood, T., Podgorney, R., Welhan, J., Mines, G., Mattson, E., Wood, R., Palmer, C. and Smith, R., 2014, David Blackwell's Forty Years in the Idaho Desert, The Foundation for 21st Century Geothermal Research; Geothermal Resources Council *Transactions*, v.38, p.143-153.

MIT, 2006, The Future of Geothermal Energy: Impact of Enhanced Geothermal Systems (EGS) on the United States in the 21st Century; Massachusetts Inst. Technology, Report INL/EXT-06-11746, 372 pp.

Moody, A., J. Fairley and M. Plummer, in prep., Designing an engineered geothermal reservoir in the welded tuffs of the Snake River Plain; *Geol. Soc. America Special Paper*.

Moos, D. and C.A. Barton, 1990, In-situ stress and natural fracturing at the INEL site, Idaho; a report to EG&G Idaho, Inc., EGG-NPR-10631.

Morgan, L.A., and W.C. McIntosh, 2005, Timing and development of the Heise volcanic field, Snake River Plain, Idaho, western USA; *Geological Society of America Bulletin*, v. 117, p. 288.

Morse, L.H. and M. McCurry, 2002, Genesis of alteration of Quaternary basalts within a portion of the eastern Snake River Plain Aquifer; in P.K. Link and L.L. Mink (eds.), Geology, hydrogeology, and environmental remediation: Idaho National Engineering and Environmental Laboratory, eastern Snake River Plain, Idaho, *Geological Society of America Special Paper* 353, p. 213-224.

Podgorney, R., M. McCurry, T. Wood, T. McLing, A. Ghassemi, J. Welhan, G. Mines, M. Plummer, J. Moore, J. Fairley and R. Wood, 2013, Enhanced Geothermal System Potential for Sites on the Eastern Snake River Plain, Idaho; Geothermal Resources Council *Transactions*, v. 37, p. 191-197.

Ramirez-Guzman, A., Y. Taran and M.A. Armienta, 2004, Geochemistry and origin of high-pH thermal springs in the Pacific coast of Guerrero, Mexico; *Geofísica Internacional*, v. 43, p. 415-425.

Reed, M.H., and Spycher, N.F., 1984, Calculation of pH and mineral equilibria in hydrothermal water with application to geothermometry and studies of boiling and dilution; *Geochim. Cosmochim. Acta*, v.48, p.1479-1490.

Ryan, J.G. and C.H. Langmuir, 1987, The systematics of lithium abundances in young volcanic rocks; *Geochim. Cosmochim. Acta*, v.51, p.1727-1741.

Ryan, J.G. and C.H. Langmuir, 1993, The systematics of boron abundances in young volcanic rocks; *Geochim. Cosmochim. Acta*, v.57, p.1489-1498.

Savov, I.P., W.P. Leeman, C.A. Lee and S.B. Shirey, 2009, Boron isotopic variations in NW USA rhyolites: Yellowstone, Snake River Plain, eastern Oregon; *J. Volcanology and Geothermal Research*, v. 188, p.162–172.

Shervais, J.W., D.R. Schmitt, D.L. Nielson, J.P. Evans, E.H. Christiansen, L. Morgan, W.C.P. Shanks, T. Lachmar, L.M. Liberty, D.D. Blackwell, J.M. Glen, D. Champion, K.E. Potter and J.A. Kessler, 2013, First results from HOTSPOT: The Snake River Plain Scientific Drilling Project, Idaho, USA; Scientific Drilling, v. 15, p. 36-45.

Smith, R.P., 2004, Geologic setting of the Snake River Plain aquifer and vadose zone; *Vadose Zone Journal*, v. 3, p. 47-58.

Twining, B.V. and J.C. Fisher, 2015, Multilevel Groundwater Monitoring of Hydraulic Head and Temperature in the Eastern Snake River Plain Aquifer, Idaho National Laboratory, Idaho, 2011–13; U.S. Geological Survey, Sci. Investigations Rept. 2015-5042, 49 pp.

Waag, C.J. and S.H. Wood, 1987, Evaluation of the Boise geothermal system; Idaho Dept. of Water Resources, Geothermal Investigations in Idaho, Final Report, 70 pp.

Wedepohl, K.H. (ed.), 1974, Handbook of Geochemistry, Springer-Verlag Berlin.

Welhan, J.A., 2012, Preliminary hydrogeologic analysis of the Mayfield area, Ada and Elmore Counties, Idaho; Idaho Geological Survey, Staff Report S-12-2, 41 pp.

Welhan, J.A., 2015, Thermal and Trace-Element Anomalies in the Eastern Snake River Plain Aquifer: Toward a Conceptual Model of the EGS Resource; Geothermal Resources Council *Transactions*, v. 39, p. 363-375.

White, D.E., 1967, Mercury and base-metal deposits with associated thermal and mineral waters; in H.L. Barnes (ed.), Geochemistry of hydrothermal ore deposits; Holt, Rinehart and Winston, NY, p. 575-631.

Whitehead, R.L., 1986, Geohydrologic framework of the Snake river Plain, Idaho and eastern Oregon; U.S. Geological Survey, Hydrologic Investigations Atlas HA-681; three plates.

Young, H.W., 1985, Geochemistry and hydrology of thermal springs in the Idaho batholith and adjacent areas, central Idaho; U.S. Geological Survey, Water Resources Investigations Report 85-4172, 44 pp.

Youngs, S.W., 1981, Geology and geochemistry of the Running Springs geothermal area, southern Bitterroot lobe, Idaho batholith; Washington State University, M.S. thesis, 125 pp.